SEGMENTATION OF ACCELEROMETER SIGNALS RECORDED DURING CONTINUOUS TREADMILL WALKING

Laurent Oudre, Alexandre Lung-Yut-Fong, Pascal Bianchi

TELECOM ParisTech
37-39 rue Dareau, 75014 Paris, France
{oudre,lung,bianchi}@telecom-paristech.fr

ABSTRACT

This paper describes a method for segmentation of triaxial accelerometer signals recorded during continuous treadmill walking. More specifically, we aim at detecting changes in speed and in incline by analyzing the accelerometer signals recorded on the shin or the waist of the walker. The raw accelerometer signals are transformed either in the time-frequency domain (with a Short-Time Fourier Transform) or in a specific features space (which emphasizes the characteristics of the gait). The transformed signals serve as inputs for change-point detection methods which output a number of estimated change times. Several change-point detection methods are tested, either parametric or non-parametric. In particular, a new change-point detection method is introduced, which takes into account the frequency structure of walking signals. The different signal representations and change-points detection methods are evaluated on a corpus of 24 subjects. An analysis of the obtained results is presented for the two considered sensors (waist and shin).

1. INTRODUCTION

The monitoring of energy expenditure (EE) can be useful in the prevention and the treatment of obese or elderly people. Even if there exist some reliable methods to evaluate the level of physical activity (such as oxygen uptake measurement or doubly labeled water), those are often expensive and intrusive and then do not suit for daily use. An alternative approach for the assessment of EE involves the use of unconstrained portable systems such as accelerometers [1].

As walking is one the most energy consuming activity in human daily life, it makes sense to evaluate the associated EE as precisely as possible. Yet, the EE strongly depends on the type of walking (speed and incline for example) [2]. Many recent works have therefore attempted to classify walking segments according to their incline or speed. This classification relies on the prior calculation of some time-domain [3, 4, 5] or time-frequency domain [4, 5, 6, 7, 8, 9] features, which emphasize the characteristics of the different types of walking. The classification is finally performed by using empirical thresholds [6, 7, 8] or classical machine learning procedures such as neural networks [3] or Gaussian Mixture Models (GMM) [4, 5, 9].

Whereas much attention has been given to the classification of walking segments, most of the publications assume that the accelerometer signals have beforehand been divided into coherent segments. Only a few works have investigated the automatic segmentation of continuous walking records [6, 8]. Furthermore, these methods only enable to segregate the level walking from the ascending or descending stairs. We here propose to divide a continuous treadmill walking record into segments where the speed and the incline are constant, by using some multiple change-points detection methods. In particular, we introduce a new multiple change-points detection method which takes into account the frequency structure of walking.

Section 2 explains the experimental protocol for the recording of the accelerometer signals. Section 3 describes the two types of signal representation we chose to use in this paper. Section 4 introduces a number of change-point detection methods, some of them new. The results obtained on our 9 subjects corpus are finally presented and explained on Section 5.

This work was funded by ANR program TECSAN-SVELTE.

Activity	Start time	End time
Level walking at 3.3 km/h	10:56:00	11:01:00
Level walking at 4.4 km/h	11:01:00	11:06:00
Level walking at 5.5 km/h	11:08:00	11:13:00
Slope walking at 4.4 km/h with 5% incline	11:14:30	11:19:30
Slope walking at 4.4 km/h with 10% incline	11:19:30	11:24:30

Table 1: Typical sequence of activities

2. EXPERIMENTAL PROTOCOL

Twenty-four healthy and consenting subjects were asked to walk on a treadmill for 20 to 25 minutes. They wore two triaxial accelerometers (MotionPod^{TM}by MOVEA): one at the shin and one at the waist. The data acquisition was performed by the Centre de Recherche en Nutrition Humaine (Rhône-Alpes) and CEA-LETI. The signals were digitized with a sampling frequency of $F_s = 100$Hz. During the experiment, either the speed or the incline of the treadmill was changed every 5 minutes (which gives 3 or 4 change points for each subject). The changes were annotated either as one time value or as two time values (in this case the change occurred between these two times). A typical annotation file is presented on Table 1. Since the sensors can sometimes be misplaced, an off-line calibration was performed in order to identify the three dimensions of the sensor: mediolateral, vertical and anteroposterior. An example of continuous walking record is presented on Figure 1.

3. SIGNAL REPRESENTATIONS

Change in speed or in incline are hardly identifiable in raw accelerometer signals. We therefore transform these raw signals either in the time-frequency domain or in a specific features domain, so as the characteristics of the gait are more visible.

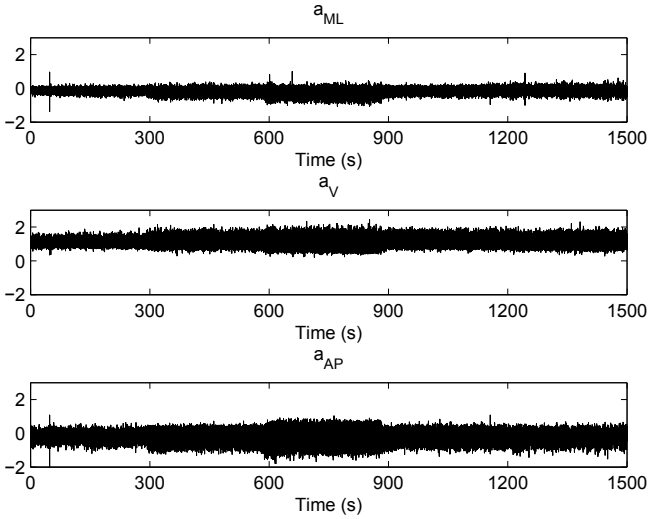

Figure 1: Example of continuous walking record. a_{ML}, a_V and a_{AP} respectively stands for the mediolateral, vertical and anteroposterior acceleration. The annotated change points are located at 300, 600, 900 and 1200 seconds. The associated speeds and inclines are the same as those presented on Table 1.

3.1 Representation A: Short-Time Fourier Transform (STFT)

In order to better identify the changes in speed and incline, we propose to work in the time-frequency domain. We chose the most common time-frequency representation of signals: the Short-Time Fourier Transform (STFT).

Let a be an accelerometer signal. Let $\mathbf{X} \in \mathbb{C}^{F \times N_f}$ be the Short-Time Fourier Transform (STFT) of a, calculated with window w of size $N_w = 1024$ and hop size $N_h = 256$. Since the frequency of walking movements are ranged from 0.6Hz to 2.5Hz [10], we only consider the frequency bins comprised between $f_{min} = 0.5$Hz and $f_{max} = 5$Hz.

While our accelerometers are able to output the acceleration in all three directions, our experiments showed that the best results were achieved by applying the STFT to the anterioposterior component.

3.2 Representation B: Features vector

Most of the walking pattern classification methods calculate specific features from the raw accelerometer signals, in order to emphasize some characteristics of the gait. Even if these features have only been used in a classification context so far, they can also be used to segment a walking record, since a change gait is likely to be reflected on the features. We decided to work on a subset of the features introduced in [4], and more specifically the 12 time-domain features they define. Note that, contrary to the STFT representation which only required one component, these features are calculated by using all three components of our accelerometers.

The signals are first divided into frames of 360 samples with an hop size of 60 samples. By denoting a_{ML}, a_V and a_{AP} respectively the mediolateral, vertical and anteroposterior acceleration, 12 time-domain features are calculated on each frame:

- mean of $a_{ML} + a_V$, a_{AP} and a_V
- standard deviation of $a_{AP} + a_V$ and a_{ML}
- median of a_V
- upper 95^{th} percentile of a_{ML}
- number of zero-crossing of a_{ML} and a_V
- cross-correlation between a_{ML}, a_{AP} and a_V.

The justification of this choice of features, as well as their interpretation in the walking context are presented in [4].

4. CHANGE POINTS DETECTION

Our aim is to detect a series of change times in either the STFT or the features matrix, which correspond to changes in speed or incline. The number of desired change points is supposed to be unknown.

4.1 Methods 1 & 2: Change in the non-centrality parameter in a multivariate noncentral chi-square distribution. Application to STFT.

4.1.1 Multiple change-point detection basics

The change point detection method we use here is adapted from the off-line estimation of change time proposed in [11], based on the generalized likelihood ratio. Consider a sequence of N independent vector-valued random observations $\{\mathbf{y}_n\}_n$ of size F. We assume that all F components are independent and that $\mathbf{y}_n$ follows a noncentral chi square distribution of non-centrality parameter $\boldsymbol{\theta}_n$ and l degrees of freedom, whose density can be written as $p_{\boldsymbol{\theta}_n}(\mathbf{y}_n)$.

Let us first describe the single change point method. Assume that there exists at most one change point in $[1:N]$. We introduce the following hypotheses:

$$\mathbf{H}_0 \quad \boldsymbol{\theta}_n = \boldsymbol{\theta} \quad 1 \leq n \leq N \tag{1}$$
$$\mathbf{H}_k \quad \boldsymbol{\theta}_n = \boldsymbol{\theta}^0 \quad 1 \leq n \leq k \tag{2}$$
$$\boldsymbol{\theta}_n = \boldsymbol{\theta}^1 \quad k+1 \leq n \leq N \tag{3}$$

There, $\boldsymbol{\theta}$, $\boldsymbol{\theta}^0$ and $\boldsymbol{\theta}^1$ are unknown, as well as the possible change point k. With the noncentral chi square distribution assumption, $\boldsymbol{\theta}$, $\boldsymbol{\theta}^0$ and $\boldsymbol{\theta}^1$ are estimated by:

$$\hat{\boldsymbol{\theta}} = \frac{1}{N}\sum_{n=1}^{N} \mathbf{y}_n - l$$

$$\hat{\boldsymbol{\theta}}^0 = \frac{1}{k}\sum_{n=1}^{k} \mathbf{y}_n - l \qquad \hat{\boldsymbol{\theta}}^1 = \frac{1}{N-k}\sum_{n=k+1}^{N} \mathbf{y}_n - l \tag{4}$$

Assume there exists one and only one change in the noncentrality parameter in $[1:N]$. Then, it means that k exists, such as $\mathbf{H}_k$ is true. This change time can be estimated as:

$$\begin{aligned}
\hat{k} &= \underset{k}{\operatorname{argmax}} \log\left[\prod_{n=1}^{k} p_{\hat{\boldsymbol{\theta}}^0}(\mathbf{y}_n) \prod_{n=k+1}^{N} p_{\hat{\boldsymbol{\theta}}^1}(\mathbf{y}_n)\right] \\
&= \underset{k}{\operatorname{argmax}} \left[\sum_{n=k+1}^{N} \log\frac{p_{\hat{\boldsymbol{\theta}}^1}(\mathbf{y}_n)}{p_{\hat{\boldsymbol{\theta}}^0}(\mathbf{y}_n)} + \sum_{n=1}^{N} \log p_{\hat{\boldsymbol{\theta}}^0}(\mathbf{y}_n)\right] \\
&= \underset{k}{\operatorname{argmax}} \sum_{n=k+1}^{N} \log\frac{p_{\hat{\boldsymbol{\theta}}^1}(\mathbf{y}_n)}{p_{\hat{\boldsymbol{\theta}}^0}(\mathbf{y}_n)}
\end{aligned} \tag{5}$$

In order to check if $\hat{k}$ is an acceptable change time, we calculate the logarithm of the generalized likelihood ratio cor-

responding to the hypotheses $\mathbf{H}_0$ and $\mathbf{H}_{\hat{k}}$:

$$M(\hat{k}) = \sum_{n=1}^{\hat{k}} \log p_{\hat{\boldsymbol{\theta}}^0}(\mathbf{y}_n) + \sum_{n=\hat{k}+1}^{N} \log p_{\hat{\boldsymbol{\theta}}^1}(\mathbf{y}_n) - \sum_{n=1}^{N} \log p_{\hat{\boldsymbol{\theta}}}(\mathbf{y}_n). \tag{6}$$

We conclude that if $M(\hat{k}) > M*$ (where $M*$ is an empirical threshold chosen as explained in Section 5.2.2), then there is a change point in $[1:N]$, and this change point is $\hat{k}$

This single change-point detection method can be extended for the estimation of multiple change-points. In this case, the change points are estimated iteratively through the Iterated Cumulative Sums of Squares Algorithm (ICSS) [12]. We first apply our single change-point detection method to the whole sequence so as to estimate the first and last change-points, and then apply iteratively the algorithm to the sequence comprised between those two points, until no other change-point is detected.

4.1.2 Method 1: Straightforward application to the STFT (classical)

Let $x_{f,n} \in \mathbb{C}$ be the STFT at frame $n \in [1:N_f]$ and frequency bin $f \in [1:F]$. Consider the distribution:

$$x_{f,n} \sim \mathscr{CN}(\mu_{f,n}, \sigma^2) \tag{7}$$

where $\mathscr{CN}(\mu, \sigma^2)$ denotes the complex circular Gaussian distribution of mean μ and variance σ^2. Then, if we write $v_{f,n} = \frac{2|x_{f,n}|^2}{\sigma^2}$ and $\theta_{f,n} = \frac{2|\mu_{f,n}|^2}{\sigma^2}$:

$$v_{f,n} \sim \chi^2\left(\theta_{f,n}, 2\right). \tag{8}$$

where $\chi^2(\theta, l)$ is the noncentral chi square distribution with non-centrality parameter θ and l degrees of freedom. Assume that all frequency components are independent. We note symbolically:

$$\mathbf{v}_n \sim \chi^2(\boldsymbol{\theta}_n, 2). \tag{9}$$

where $\mathbf{v}_n = [v_{1,n}, \cdots, v_{F,n}]'$ and $\boldsymbol{\theta}_n = [\theta_{1,n}, \cdots, \theta_{F,n}]'$.

Method 1 consists in the application of the change-point detection algorithm described in Section 4.1.1 to the sequence $\{\mathbf{v}_n\}_n$. Note that, in order to compute $\mathbf{v}_n$, we need to know the value of σ^2. This value is estimated by calculating the variance of $\mathbf{X}$ for frequency bins which stand outside of the peak values of the spectrogram.

4.1.3 Method 2: Frequency model of the STFT (structured)

The STFT calculated on walking periods tends to show a strong harmonic structure (see Figure 2). Each spectrogram frame can therefore be modeled by peaks located at each integer-multiple of a fundamental frequency bin f_0. If the width of the main lobe of window w is lower than $\frac{f_0}{2}$, we can assume that there is no overlap between the contributions of each harmonic. We introduce the following model:

$$\mathbb{E}\left[v_{f,n}\right] = \sum_{h=1}^{H} \rho_{h,n} |W(f - hf_0)|^2 \tag{10}$$

where $W(f)$ is the Fourier transform of window w, H the number of harmonics (which value is determined by f_{max} and f_0) and $\rho_{h,n}$ is the magnitude of harmonic h on frame n. Under this model, the parameter $\hat{\theta}^0$ calculated in (4) is now *structured* and entirely determined by $\hat{f}^0$ (frequency bin of the main peak in the averaged spectrogram) and $\left\{\hat{\rho_h}^0\right\}_h$ (magnitude of the averaged spectrogram at integer-multiple values of $\hat{f}^0$) such as:

$$\hat{f}^0 = \underset{f}{\operatorname{argmax}} \frac{1}{k} \sum_{n=1}^{k} v_{f,n} \qquad \hat{\rho_h}^0 = \frac{1}{k} \sum_{n=1}^{k} v_{h\hat{f}^0,n} \tag{11}$$

The same process can be used to estimate θ^1 and θ.

Method 2 is therefore an adaptation of the algorithm previously described, taking into account the particularity of the spectrogram structure. The only difference between this method and the previous one lies in the estimation of $\hat{\theta}^0$ and $\hat{\theta}^1$ in (4).

4.2 Method 3: Non-parametric rank-based multivariate change-point detection (dynMKW)

The non-parametric method we consider here is introduced and described in [13]. Note that this method can either be applied on the STFT or on the features matrix and that it makes no assumption on the underlying distribution of the observations. Also, contrary to methods 1&2, this approach is parameter-free.

Let $\{\mathbf{y}_n\}_n$ be a sequence of N F-dimensional random observations. Suppose that there exist $K-1$ change points in $[1:N]$, which will be written $k_1, \cdots, k_{K-1}$ with $k_0 = 0$ and $k_K = N$. Introduce

$$r_{f,n} = \sum_{n'=1}^{N} \mathbf{1}_{\{y_{f,n'} \leq y_{f,n}\}} - \frac{N}{2} \tag{12}$$

whose first term represents the rank of $y_{f,n}$ and

$$\bar{r}_{f,j} = \frac{1}{k_{j+1} - k_j} \sum_{n=k_j+1}^{k_{j+1}} r_{f,n} \tag{13}$$

the average rank of the jth group in the fth dimension.

Define the statistic

$$T(k_1, \ldots, k_{K-1}) = \frac{1}{N^2} \sum_{j=0}^{K-1} (k_{j+1} - k_j) \bar{\mathbf{r}}_j' \, \hat{\Sigma}^{-1} \, \bar{\mathbf{r}}_j \,, \tag{14}$$

where $\bar{\mathbf{r}}_j = \left[\bar{r}_{1,j}, \cdots, \bar{r}_{F,j}\right]'$ and $\hat{\Sigma}$ is a $F \times F$ matrix defined by:

$$\hat{\Sigma}_{f,f'} = \frac{1}{N^2} \sum_{n=1}^{N} r_{f,n} r_{f',n}. \tag{15}$$

If we suppose that the number of change-points is known and that the signal can be segmented into K groups, the change-points locations can be estimated by maximizing (14):

$$(\hat{k}_1, \ldots, \hat{k}_{K-1}) = \underset{0 < k_1 < \cdots < k_{K-1} < N}{\operatorname{argmax}} T(k_1, \ldots, k_{K-1}). \tag{16}$$

Obviously, computing the statistic for all possible values of the potential location of the segment boundaries has a prohibitive computational cost. Given the additive characteristic of the objective function, it can nonetheless be done in an efficient manner using a dynamic programming algorithm [14].

The number of segments in the signal is estimated heuristically by using a method described in [13].

4.3 Method 4: Change in the mean of a multivariate Gaussian distribution (dynGAU)

This method is an adaptation of the one presented in Section 4.2, in the case where data is assumed to be Gaussian.

Let us write $\tilde{\mathbf{y}}_n = \mathbf{y}_n - \sum_{n'=1}^{N} \mathbf{y}_{n'}$. Then, the test statistic described in (14) is now computed by replacing $\bar{r}_{f,j}$ in (13) by:

$$\bar{r}_{f,j} = \frac{1}{k_{j+1} - k_j} \sum_{n=k_j+1}^{k_{j+1}} \tilde{y}_{f,n} \tag{17}$$

and $\hat{\Sigma}_{f,f'}$ in (15) by:

$$\hat{\Sigma}_{f,f'} = \frac{1}{N^2} \sum_{n=1}^{N} \tilde{y}_{f,n} \tilde{y}_{f',n}. \tag{18}$$

The estimation method is the same as with *dynMKW*.

5. RESULTS

5.1 Comparison between Methods 1 & 2

An example of change-point detection in the STFT (Methods 1 & 2) is presented on Figure 2. We see that only Method 2 (structured), when applied to the shin sensor, is able to detect all four annotated change points. All the other methods only detect the three first ones, which involve a change in speed (easily visible in the time-frequency domain as with a constant step length, a change of speed corresponds to a change in frequency). On the contrary, a change in incline does not seem to involve a change in frequency, but rather a change in the magnitudes of the harmonics. Then, it seems logical that Method 2, which explicitly evaluates these magnitudes, better detects the changes in incline. The better results obtained with the shin sensor can be explained by the fact that the first harmonic of the waist signal has a very low amplitude (degrading the evaluation of the fundamental frequency), while the higher harmonics tend to oscillate (degrading the evaluation of the magnitudes of the harmonics).

5.2 General results

5.2.1 Metrics

In order to evaluate our different approaches, we compare the output sequence of detected change times to the annotations. Let us remind that as described in Section 2 and Table 1, our change times are either annotated as one or two times. Since these annotations are not perfect, we need to introduce some tolerance for the evaluation. We use the following conventions (times are given in seconds):

- If the change point is annotated as one time t, the detected change point $\hat{t}$ is correct if $\hat{t} \in [t-30 : t+30]$.
- If the change point is annotated as two times $[t_1 : t_2]$, the detected change point is correct if $\hat{t} \in [t_1 - 10 : t_2 + 10]$

We then compute two scores: the precision and the recall, defined as follows:

- If among the $\hat{K}$ detected change points, only $\hat{C}$ are correct, the precision is defined as $p = \frac{\hat{C}}{\hat{K}}$.
- If among the K ground truth change points, only C are correctly detected, the recall is defined as $r = \frac{C}{K}$

Those scores are then averaged among all the subjects of the corpus.

		Waist		Shin	
		p	r	p	r
(A) STFT	(1) classical	0.50	**0.72**	0.49	0.77
	(2) structured	0.46	0.65	0.49	**0.79**
	(3) dynMKW	0.50	0.67	0.51	0.71
	(4) dynGAU	0.50	0.63	0.47	0.61
(B) Features	(3) dynMKW	0.51	0.69	0.57	**0.79**
	(4) dynGAU	0.49	0.66	0.57	0.73

Table 2: Precision and recall obtained on the 24 subjects corpus

5.2.2 Results

The precisions and recalls obtained with the different sensors, signal representations and change-point detection methods are displayed on Table 2. The empirical threshold used in Methods 1 & 2 has been chosen so as to give a precision approximately equal to 0.50 (which is the average precision value of Methods 3 & 4).

Representation A (STFT) Concerning Methods 1 & 2, these results tend to confirm the assumptions made in Section 5.1. Indeed, the recall scores are always higher with the shin sensor (whose STFT has a clearer structure than the waist one) and the introduction of the frequency structure improves the scores when using the shin sensor. It is interesting to notice that when working with the shin sensor, the best recall is obtained by using a method with a dedicated model (structured). On the contrary, since the STFT calculated on the waist signals shows some properties which do not fit our model (oscillating harmonics, low magnitudes of the fundamental frequencies), the best recall is obtained with a non-parametric method (dynMKW) or a more generic method (classical).

Representation B (Features) When working with representation B, the non-parametric method 3 performs better that the parametric one. This can be due by the fact that the Gaussian assumption does not fit the reality of these signals. Also, Method 4 only detects changes in mean but in reality it is more likely that these changes may occur in mean and variance.

6. CONCLUSION

We have presented and evaluated several approaches for the segmentation of accelerometers signals recorded during continuous treadmill walking. On our corpus composed of 24 subjects, 72% of the changes in speed of incline were correctly detected when working on waist signals, and 79% on the shin signals. A straightforward perspective would be to adapt and test these methods on real-life walking records, where the changes in speed and incline are smoother than on a treadmill. Also, this study could be extended to a larger set of subjects, in order to better investigate the limits of our systems.

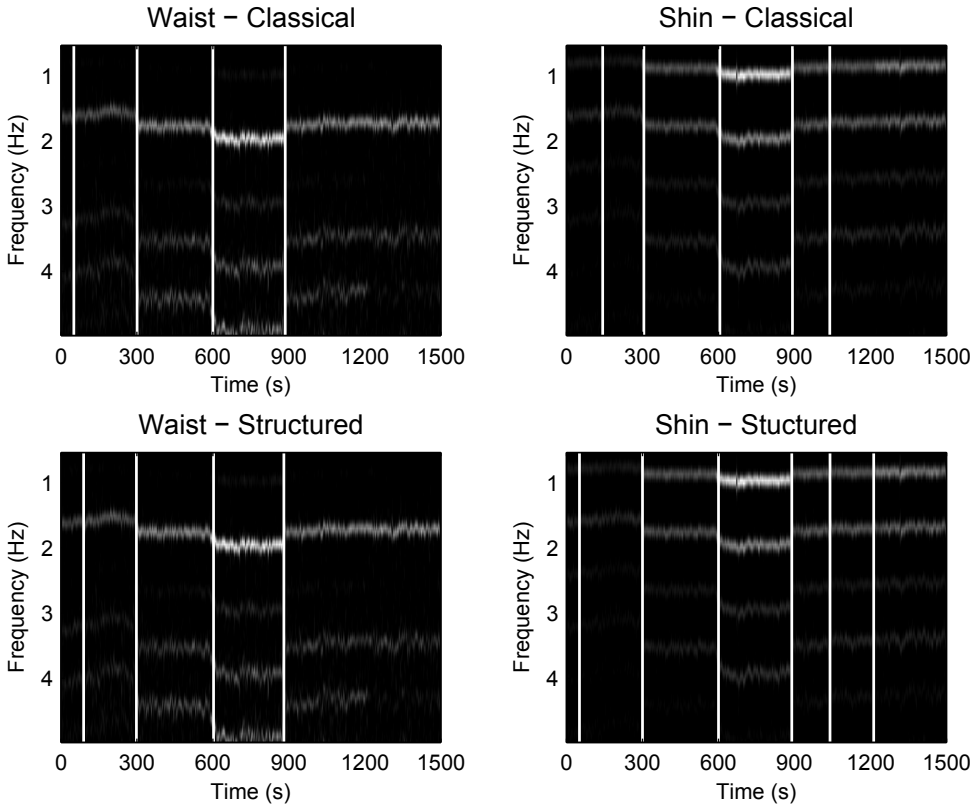

Figure 2: Change point detection in the Short-Time Fourier Transform with methods 1 & 2 and sensors waist and shin. The annotated change points are located at 300, 600, 900 and 1200 seconds. The two first change points correspond to a change in speed, the third one to a change in speed and incline and the last one to a change in incline.

REFERENCES

[1] C. Bouten, K. Koekkoek, M. Verduin, R. Kodde, and J. Janssen, "A triaxial accelerometer and portable data processing unit for the assessment of daily physical activity," *IEEE Transactions on Biomedical Engineering*, vol. 44, no. 3, pp. 136–147, 1997.

[2] P. Terrier, K. Aminian, and Y. Schutz, "Can accelerometry accurately predict the energy cost of uphill/downhill walking?" *Ergonomics*, vol. 44, no. 1, pp. 48–62, 2001.

[3] K. Aminian, P. Robert, E. Jequier, and Y. Schutz, "Estimation of speed and incline of walking using neural network," *IEEE Transactions on Instrumentation and Measurement*, vol. 44, no. 3, pp. 743–746, 1995.

[4] N. Wang, E. Ambikairajah, S. Redmond, B. Celler, and N. Lovell, "Classification of walking patterns on inclined surfaces from accelerometry data," in *Proceedings of the International Conference on Digital Signal Processing (DSP)*, 2009, pp. 1–4.

[5] N. Wang, S. Redmond, E. Ambikairajah, B. Celler, and N. Lovell, "Can triaxial accelerometry accurately recognize inclined walking terrains?" *IEEE Transactions on Biomedical Engineering*, vol. 57, no. 10, pp. 2506–2516, 2010.

[6] M. Sekine, T. Tamura, T. Togawa, and Y. Fukui, "Classification of waist-acceleration signals in a continuous walking record," *Medical Engineering & Physics*, vol. 22, no. 4, pp. 285–291, 2000.

[7] M. Sekine, T. Tamura, M. Akay, T. Fujimoto, T. Togawa, and Y. Fukui, "Discrimination of walking patterns using wavelet-based fractal analysis," *IEEE Transactions on Neural Systems and Rehabilitation Engineering*, vol. 10, no. 3, pp. 188–196, 2002.

[8] M. Nyan, F. Tay, K. Seah, and Y. Sitoh, "Classification of gait patterns in the time-frequency domain," *Journal of Biomechanics*, vol. 39, no. 14, pp. 2647–2656, 2006.

[9] R. Ibrahim, E. Ambikairajah, B. Celler, and N. Lovell, "Time-frequency based features for classification of walking patterns," in *Proceedings of the International Conference on Digital Signal Processing (DSP)*, 2007.

[10] M. Henriksen, H. Lund, R. Moe-Nilssen, H. Bliddal, and B. Danneskiod-Samsře, "Test-retest reliability of trunk accelerometric gait analysis," *Gait & Posture*, vol. 19, no. 3, pp. 288–297, 2004.

[11] M. Basseville and I. Nikiforov, *Detection of abrupt changes: theory and application*. Prentice-Hall, Inc., 1993, ch. 2.6 - Off-line change detection, pp. 57–61.

[12] C. Inclan and G. Tiao, "Use of cumulative sums of squares for retrospective detection of changes of variance," *Journal of the American Statistical Association*, vol. 89, no. 427, pp. 913–923, 1994.

[13] A. Lung-Yut-Fong, C. Lévy-Leduc, and O. Cappé, "Robust retrospective multiple change-point estimation for multivariate data," *ArXiv e-prints (1102.1796)*, 2011.

[14] S. Kay, *Fundamentals of statistical signal processing: detection theory*, 1993.